



Publication Year	2016
Acceptance in OA @INAF	2020-05-20T10:58:40Z
Title	Model supporting the use of pressure in the hot slumping of glass substrates for X-ray telescopes
Authors	SALMASO, Bianca; Brizzolari, Claudia; SPIGA, Daniele
DOI	10.1364/OE.24.024799
Handle	http://hdl.handle.net/20.500.12386/24993
Journal	OPTICS EXPRESS
Number	24

Model supporting the use of pressure in the hot slumping of glass substrates for X-ray telescopes

BIANCA SALMASO,^{1,*} CLAUDIA BRIZZOLARI,² AND DANIELE SPIGA¹

¹INAF/Brera Astronomical Observatory, Via E. Bianchi 46, 23807 Merate, Italy

²Università degli Studi dell'Insubria, Via Valleggio 11, 22100 Como, Italy

*bianca.salmaso@brera.inaf.it

Abstract: Thin glass foils are nowadays considered good substrates for lightweight focusing optics, especially for X-ray telescopes. The desired shape can be imparted to the foils by hot slumping, a process that replicates the shape of a slumping mould. During thermal slumping, when the glass and the mould come into contact, ripples in the glass surface appear spontaneously if the thermal expansions are mismatched. In our hot slumping setup, pressure is applied to ease the mould shape replication and to enhance the ripple relaxation. Starting from an existing model developed to explain the ripple formation in hot-slumped glass foils without pressure, we have developed a model that includes the pressure to support our experimental results.

© 2016 Optical Society of America

OCIS codes: (340.7470) X-ray mirrors; (220.4610) Optical fabrication; (160.2750) Glass and other amorphous materials.

References and links

1. J. E. Koglin, C. M. Hubert Chen, J. Chonko, F. E. Christensen, W. W. Craig, T. R. Decker, K. S. Gunderson, C. J. Hailey, F. A. Harrison, C. P. Jensen, K. K. Madsen, M. Stern, D. L. Windt, H. Yu, and E. Ziegler, "Production and calibration of the first HEFT hard X-ray optics module," *Proc. SPIE* **5168**, 100 (2004).
2. W. W. Craig, H. J. An, K. L. Blaedel, F. E. Christensen, T. A. Decker, A. Fabricant, J. Gum, C. J. Hailey, L. Hale, C. B. Jensen, J. E. Koglin, K. Mori, M. Nynka, M. J. Pivovarov, M. V. Sharpe, M. Stern, G. Tajiri, and W. W. Zhang, "Fabrication of the NuSTAR Flight Optics," *Proc. SPIE* **8147**, 81470H (2011).
3. W. W. Zhang, K.-W. Chan, T. Hajimichael, J. P. Lehan, S. Owens, R. Petre, T. T. Saha, M. Gubarev, W. D. Jones, and S. L. O'Dell, "Development of Lightweight X-Ray Mirrors for the Constellation-X Mission," *Proc. SPIE* **6688**, 668811 (2007).
4. W. W. Zhang, M. Atanassova, M. Biskach, P. N. Blake, G. Byron, K. W. Chan, T. Evans, C. Fleetwood, M. Hill, M. Hong, L. Jalota, L. Kolos, J. M. Mazzarella, R. McClelland, L. Olsen, R. Petre, R. Robinson, T. T. Saha, M. Sharpe, M. V. Gubarev, W. D. Jones, T. Kester, S. L. O'Dell, D. Caldwell, W. Davis, F. Freeman, W. Podgorski, P. B. Reid, and S. Romaine, "Mirror Technology Development for the International X-ray Observatory Mission (IXO)," *Proc. SPIE* **6688**, 668811 (2007).
5. G. Pareschi, S. Basso, M. Bavdaz, O. Citterio, M. M. Civitani, P. Conconi, D. Gallieni, D. Martelli, G. Parodi, L. Proserpio, G. Sironi, D. Spiga, G. Tagliaferri, M. Tintori, E. Wille, and A. Zambra, "IXO glass mirrors development in Europe," *Proc. SPIE* **8147**, 81470L (2011).
6. A. Winter, M. Vongehr, and P. Friedrich, "Light weight optics made by glass thermal forming for future x-ray telescopes," *Proc. SPIE* **7732**, 77320B (2010).
7. B. Salmaso, C. Brizzolari, S. Basso, M. M. Civitani, M. Ghigo, G. Pareschi, D. Spiga, G. Tagliaferri, and G. Vecchi, "Slumped Glass Optics for X-ray telescopes: advances in the hot slumping assisted by pressure," *Proc. SPIE* **9603**, 96030O (2015).
8. P. B. Reid, T. L. Aldcroft, R. Allured, V. Cotroneo, R. L. Johnson-Wilke, V. Marquez, S. McMuldroy, S. L. O'Dell, B. D. Ramsey, D. A. Schwartz, S. E. Troler-McKinstry, A. A. Vikhlinin, R. H. T. Wilke, and R. Zhao, "Development status of adjustable grazing incidence optics for 0.5 arcsecond X-ray imaging," *Proc. SPIE* **9208**, 920807 (2014).
9. M. Civitani, S. Basso, M. Ghigo, G. Pareschi, B. Salmaso, D. Spiga, G. Tagliaferri, G. Vecchi, V. Burwitz, G. D. Hartner, and B. Menz, "X-ray Optical Units made of glass: achievements and perspectives," *Proc. SPIE* **9144**, 914416 (2014).
10. B. Salmaso, C. Brizzolari, S. Basso, M. M. Civitani, M. Ghigo, J. Holyszko, D. Spiga, G. Vecchi, and G. Pareschi, "Slumped Glass Optics development with pressure assistance," *Proc. SPIE* **9905**, 990523 (2016).
11. M. Ghigo and L. Proserpio, "A process for manufacturing an optical element by hot forming a glass sheet using pressure difference," International Patent Publication Number WO2015/022643.
12. B. Salmaso, S. Basso, C. Brizzolari, M. Civitani, M. Ghigo, G. Pareschi, D. Spiga, G. Tagliaferri, and G. Vecchi, "Direct hot slumping of thin glass foils for future generation X-ray telescopes: current state of the art and future outlooks," *Proc. ICSO 2014* (2015).

13. Y. Chen, "Thermal forming process for precision freeform optical mirrors and micro glass optics," PhD thesis, The Ohio State University (2010).
14. Y. M. Stokes, "Very viscous flows driven by gravity, with particular application of slumping of molten glass," Ph.D. thesis, The University of Adelaide (1998).
15. M. A. Jiménez-Garate, C. J. Hailey, W. W. Craig, and F. E. Christensen, "Thermal forming of glass microsheets for x-ray telescope mirror segments," *Appl. Optics* **42**, 4 (2003).
16. G. S. Fulcher, "Analysis of recent measurements of the viscosity of glasses," *J. Am. Cer. Soc.* **8** (6), 339 (1925).

1. Introduction

Thermal forming of thin glass foils is a technique currently used to produce lightweight X-ray mirrors with any curvature, by replication of a reference shape. Thermally-formed glass optics for X-ray astronomical mirrors were firstly introduced for the small size hard X-ray optics of the HEFT (High Energy Focusing Telescope) balloon-borne experiment [1], and more recently used for the NuSTAR mission [2]. Based on these successful applications, the thermal slumping of glass foils is considered a promising method to fabricate focusing mirrors at an affordable cost. Concerning large X-ray optics, thermal slumping of segmented glass mirrors was first studied for the Constellation-X project [3] and then for the IXO mission, both by NASA [4] and in Europe [5,6], and was thereby considered a viable alternative for the ATHENA mission [7], in addition to the baseline solution based on Silicon Pore Optics (SPO). Finally, the application of piezo-electric actuators to slumped thin glass foils, in order to reach sub-arcsecond resolution, is studied in the context of the X-ray Surveyor mission, and it is developed by the SAO/CfA in USA [8]. Clearly, aiming to reach higher angular resolution requirements, the quality of the optics has to be improved in terms of profile errors and microroughness. Many laboratories worldwide are at work to reach this goal, using different thermal slumping approaches. In our laboratories we have produced several prototypes [9], working from 2009 until 2013 under ESA contract. Since then, the process was improved to reduce low-, mid- and high-frequency errors in the profile of the slumped glass foils [10]. The best results were obtained coupling the Corning Eagle XG glass with the Schott Zerodur K20, owing their very similar Coefficient of Thermal Expansion ($CTE_{\text{Eagle}} = 3.17 \times 10^{-6} / \text{K}$, $CTE_{\text{K20}} = 2.2 \times 10^{-6} / \text{K}$). Eagle glass foil, 0.4 mm thick, is slumped over a convex cylindrical mould in K20, and trimmed to the final size of $200 \times 200 \text{ mm}^2$. We have adopted a direct slumping configuration, in which the optical surface of the glass is the one in contact with the mould, in order to have the mirror profile unaffected by the thickness variation in the glass foils. With respect to other groups, our innovation is in the application of pressure to assist the mould replica (INAF patent WO2015/022643 [11]). A pressure of 50 g/cm^2 (about 4900 Pa) was experimentally demonstrated to be essential to minimize the mid-frequency errors of the slumped foil [12]. In this paper we present a model to support the importance of pressure in the hot slumping technology. This model extends, with the application of pressure, an existing theoretical approach [15], originally developed to explain the corrugations experimentally observed in the glass foils slumped during the HEFT glass substrates fabrication at Columbia University.

2. Modelling ripple relaxation in glass

During thermal slumping, if the glass and the mould get into contact, ripples in the glass surface are formed. Several mechanisms contribute to the formation and relaxation of ripples, and their modelling is quite complex. For instance, we have observed the presence of air bubbles entrapped between the mould and the glass when no pressure was applied, as well as an increase in ripple height when using glass and mould materials with increased CTE mismatch. On the other hand, we have observed a better relaxation of the ripples when using soaking and cooling times sufficiently long. The friction between the two surfaces would also play a key role, as a lower friction would reduce the ripples formation. To describe relaxation in glass thermal

forming different approaches can be used. Finite Element Methods were used implementing for instance the Tool-Narayanaswamy model [13] or the Stokes creeping-flow model [14]. We have used an analytical model proposed in 2003 by Jiménez-Garate [15], which simply describes the origin of the corrugations experimentally observed in our slumped glass foils, typically over spatial frequencies of 1-2 cm. In this simplified model, only the gravity and the surface tension are considered to relax the ripples, and the relaxation time is computed analytically. We have subsequently modified the model to include the pressure.

2.1. The Jiménez-Garate model without pressure

We hereafter recapitulate the derivation of Jiménez-Garate's results. The formation and relaxation of ripples involves a high number of parameters, some of which are not included in the model for simplicity reasons, such as mould figure errors, dust particles or air entrapped between the mould and the glass surface, non uniform temperature within the mould and the glass.

We consider a glass sheet with ripples, as displayed in Fig. 1, where λ is the wavelength of the ripple, a its amplitude (with $a \ll \lambda$), R its radius of curvature, $h = 2a$ is the peak-to-valley value of the ripple. The ripple profile can be described by a sinusoidal function:

$$u(x) = \frac{h}{2} \sin\left(\frac{2\pi}{\lambda}x\right). \quad (1)$$

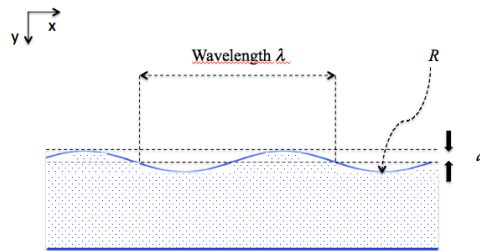


Fig. 1. A glass sheet with ripples on the surface in contact with the mould. Dimensions not in scale.

Once generated by CTE mismatch between glass and mould, the ripples tend to relax under the action of two forces:

1. **Surface tension:** from geometrical considerations, we have $(\lambda/4)^2 = (2R - a)a \sim 2Ra$, and therefore the radius R of the ripple can be written as $R \sim \lambda^2/32a$. From surface tension theory, there is an increase in pressure beneath the convex ripple equal to S/R , where S is the surface tension of the air-glass interface, and a decrease in pressure beneath the adjacent concave ripple. A differential pressure of magnitude $2S/R \sim 64aS/\lambda^2$ therefore acts to make the glass flow from the thicker to the thinner regions.
2. **Gravity:** between the thicker and the thinner locations of the glass there is a differential hydrostatic pressure $\rho gh = 2\rho ga$, where ρ is the glass density and g is the gravity acceleration.

These two forces act to reduce the ripple height, with a force per unit area given by

$$\frac{F}{A} = \frac{64aS}{\lambda^2} + 2\rho ga. \quad (2)$$

By integration of Eq. (2) in da over the local height of the profile, we have the potential energy per unit area:

$$\frac{U}{A}(x) = \int_0^u \left(\frac{64S}{\lambda^2} + 2\rho g \right) ada = \left(\frac{64S}{\lambda^2} + 2\rho g \right) \frac{u^2(x)}{2}, \quad (3)$$

and the potential energy per unit area, averaged over a sinusoidal period, is

$$\left\langle \frac{U}{A}(x) \right\rangle = \left(\frac{8S}{\lambda^2} + \frac{\rho g}{4} \right) h^2 \left\langle \sin^2 \left(\frac{2\pi}{\lambda} x \right) \right\rangle = \left(\frac{8S}{\lambda^2} + \frac{\rho g}{4} \right) \frac{h^2}{2}. \quad (4)$$

The energy stored in the ripple is dissipated via viscosity forces. In most glass forming processes, the glass can be considered a Newtonian fluid, which means that the viscous force is expressed by the formula

$$\frac{F_{yx}}{A} = \eta \frac{dv_y}{dx}, \quad (5)$$

where η is the the viscosity coefficient, F_{yx} is a force in the y direction exerted onto a surface perpendicular to the x direction and v_y is the velocity in the y direction (see the axes orientation in Fig. 1). The dissipated energy per unit area in a time dt can be written as:

$$\frac{dU}{A} = \frac{F_{yx}dy}{A} = \eta \frac{dv_y}{dx} dy = \eta \frac{dv_y}{dx} v_y dt = \frac{d}{dx} \left(\frac{1}{2} \eta v_y^2 \right) dx. \quad (6)$$

Since the relaxation process is extremely slow, we can replace the differentials with finite differences: hence we set dt equal to the relaxation time τ , $dx = \lambda$, and $dy = h$, leading to

$$\frac{U}{A} = \frac{\eta h^2}{2\tau\lambda}. \quad (7)$$

Equating Eq. (7) and Eq. (4) therefore provides the relaxation time τ as a function of the viscosity coefficient η , of the surface tension S and of the ripple spatial wavelength λ :

$$\tau = \frac{\eta}{8S/\lambda + \rho g \lambda/4}. \quad (8)$$

We note that, in this case, τ does not depend on the ripple height h . This will be, however, no longer true if the pressure is included.

2.2. Including the pressure in the model

We now include the pressure P in the model. This changes Eq. (2) into

$$\frac{F}{A} = \frac{64aS}{\lambda^2} + 2\rho ga + P, \quad (9)$$

which, by integration, returns the potential energy stored in a ripple:

$$\frac{U}{A} = \frac{8Sh^2}{\lambda^2} + \frac{\rho gh^2 + 2Ph}{4}. \quad (10)$$

The ripple relaxation time of Eq. (8) thus changes to:

$$\tau = \frac{\eta}{8S/\lambda + \rho g \lambda/4 + P\lambda/2h}, \quad (11)$$

and we see that τ expression has now an additional term $P\lambda/2h$ in the denominator. The relaxation time depends now on the ripple height h and the applied pressure P . As expected, the application of pressure reduces the relaxation time.

3. The application of the model, with and without pressure

Jiménez-Garate reports [15] rippling in AF45 and D263 glass types using steel, graphite and quartz slumping moulds. Instead, in our case, we have shown the presence of ripples with Eagle glass type using a K20 mould. In order to apply the model and compute the relaxation time τ , it is essential to have reliable data for the surface tension $S = S(T)$ and the viscosity $\eta = \eta(T)$ of the glass at the slumping temperatures.

For the Eagle glass, the S value was supplied by Corning ($S = 0.328 \text{ J/m}^2$ at $T = 1400^\circ\text{C}$, private communication). Owing to the weak dependence of S on T , we have used this value in the computation of the relaxation time: using lower values, our result was not substantially changed. On the other hand, the viscosity dependence on T is very pronounced. The $\eta(T)$ function can be computed by fitting the tabulated values reported in the data sheet (Table 1), with the Vogel-Fulcher-Tammann (VFT) formula [16]:

$$\log_{10} \eta = -A + \frac{B}{T - T_0}, \quad (12)$$

where A , B , T_0 are constants characteristic of the glass species. In our work, Eagle glass foils are slumped at 750°C , which corresponds to a viscosity value $\eta = 10^{10.95} \text{ Pa}\cdot\text{s}$, maintained for a 4 h time.

Table 1. Some key parameters of the Eagle glass used in our work.

	Density	Softening Point	Annealing Point	Strain Point	Surface Tension
Eagle	2.38 g/cm ³	971 °C	722 °C	669 °C	0.328 J/m ²

Figure 2 shows the relaxation time, τ , as a function of the ripple wavelength, λ , computed for the Eagle glass using Eq. (11). The trends of τ without (black lines) and with pressure (coloured lines) are displayed at two temperatures: the *soaking* (750°C) and the *annealing* (722°C) temperatures, that are maintained for a few hours throughout our slumping cycle.

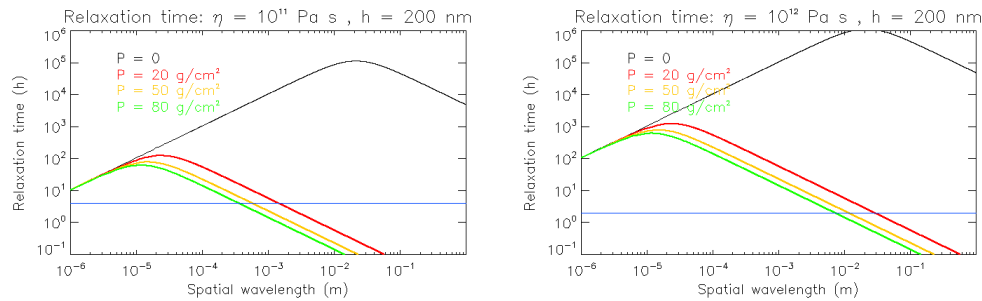


Fig. 2. Predicted relaxation time of surface ripples versus ripple wavelength, for Eagle glass: ripple heights of 200 nm are considered. The black line corresponds to the prediction without pressure. The red, orange and green lines correspond to the predictions for $P = 20$, 50, and 80 g/cm², respectively. Left: $\eta = 10^{11} \text{ Pa}\cdot\text{s}$ ($T_{\text{soak}} = 750^\circ\text{C}$), the blue line corresponds to a 4 h time. Right: $\eta = 10^{12} \text{ Pa}\cdot\text{s}$ ($T_{\text{ann}} = 722^\circ\text{C}$), the blue line marks a 2 h time.

Figure 2-left (750°C) shows that only the ripples in the λ range *below* the blue line are effectively smoothed out. Hence, ripples in the centimetre range of λ are not relaxed without pressure application in both situations. In contrast, in the model with pressure, ripples created in the centimetre spatial wavelength range are relaxed only at the higher temperature (i.e., lower

viscosity) and within a 4 h timescale. This explains why a long time is needed to allow the ripples to smooth down: based on this result, we have adopted a slow cooling time around the annealing temperature (722 °C), improving in this way the optical surface of our glass foils.

4. Comparison with experiments

Three different pressure values were used to form three Eagle glass foils: E11 was slumped with $P = 20 \text{ g/cm}^2$, E5 with $P = 50 \text{ g/cm}^2$, and E17 with $P = 80 \text{ g/cm}^2$. After forming, profile measurements of these foils were taken with the Long Trace Profilometer (LTP) and analyzed in terms of Power Spectral Density (PSD). The PSD values computed are consistent with the prediction of the models (see Fig. 3), showing decreasing amplitude of profile defects as the pressure is increased: the application of pressure diminishes the time needed for the ripples to smooth down.

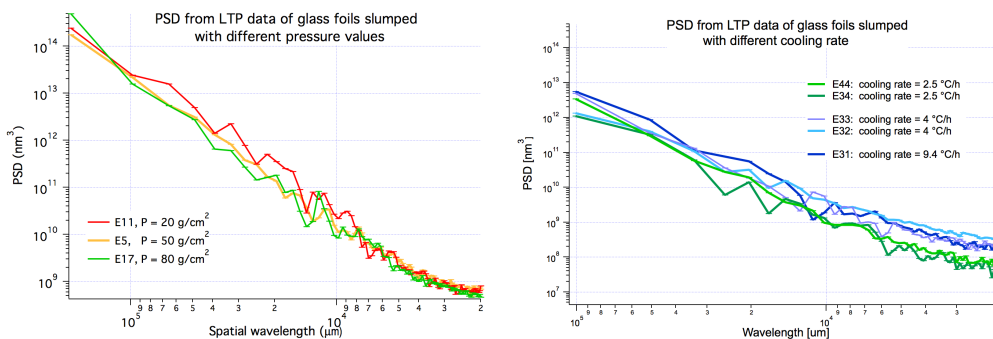


Fig. 3. Left: PSD from LTP data for Eagle glass foils slumped at different pressure values. The experimental result is consistent with the prediction of the models (see Fig. 2), showing decreasing PSD values as the pressure is increased. Right: PSD from the central $100 \times 100 \text{ mm}^2$ LTP data for Eagle glass foils slumped with the same pressure (and therefore constant τ), but different cooling rates around the annealing temperature. The gradual relaxation of the PSD in time is apparent especially in the centimetre range.

Fig. 2-right shows that the relaxation of ripples in the cm range becomes critical, even with pressure, as the temperature decreases. To compare this result with experiments, Eagle glass foils were slumped at a constant pressure value of 50 g/cm^2 , but different cooling rates to monitor the progressive relaxation of the ripples formed around the annealing temperature. The rate was decreased from 9.4 to 2.5 °C/h, and (Fig. 3-right) the PSD improvement with decreasing cooling rate is clearly seen. This shows that the ripple smoothing is a gradual phenomenon over time, which can be abridged by pressure application on the glass foil.

5. Conclusion

Hot slumping of thin glass foils is a replication technique developed in several laboratories worldwide, to produce lightweight and high angular resolution substrates for X-ray telescopes. The innovation introduced in INAF/OAB laboratories is the use of pressure to assist the replica of the mould figure. The use of pressure was experimentally observed to be essential to reduce mid-frequency errors in the profile of slumped glass foils, which crucially degrade the performances of the optics. In this paper we have supported our experimental results with a theoretical approach: starting from an existing formalism developed to explain the ripples formation in slumped glass foils [15] we have accounted for the pressure in the model, showing the pressure to be essential to relax the observed ripples, and giving us the indication to reduce the cooling rate around the annealing temperature, where the relaxation is slower owing to larger viscosity values.